Journal of Renewable Materials

Tech Science Press

DOI: 10.32604/jrm.2023.029454

ARTICLE

Naturally Nitrogen-Doped Biochar Made from End-of-Life Wood Panels for SO_2 Gas Depollution

Hamdi Hachicha[1,2], Mamadou Dia[2], Hassine Bouafif[2], Ahmed Koubaa[1], Mohamed Khlif[3] and Flavia Lega Braghiroli[1,*]

[1]Research Forest Institute (Institut de Recherche sur les Forêts, IRF), University of Québec in Abitibi-Témiscamingue (UQAT), Rouyn-Noranda, QC J9X 5E4, Canada

[2]Technology Center for Industrial Waste (Centre Technologique des Résidus Industriels, CTRI), College of Abitibi-Témiscamingue (Cégep de L'Abitibi-Témiscamingue), Rouyn-Noranda, QC J9X 5E5, Canada

[3]École D'ingénieur de Sfax, Université de Sfax, Sfax, 3038, Tunisia

[*]Corresponding Author: Flavia Lega Braghiroli. Email: Flavia.Braghiroli2@uqat.ca

Received: 20 February 2023 Accepted: 28 March 2023 Published: 31 October 2023

ABSTRACT

Reconstituted wood panels have several advantages in terms of ease of manufacturing, but their shorter life span results in a huge amount of reconstituted wood panels being discarded in sorting centers yearly. Currently, the most common approach for dealing with this waste is incineration. In this study, reconstituted wood panels were converted into activated biochar through a two-step thermochemical process: (i) biochar production using pilot scale fast pyrolysis at 250 kg/h and 450°C; and (ii) a physical activation at three temperatures (750°C, 850°C and 950°C) using an in-house activation furnace (1 kg/h). Results showed that the first stage removed about 66% of the nitrogen from the wood panels in the form of NO, NH_3, and trimethylamine, which were detected in small amounts compared to emitted CO_2. Compared to other types of thermochemical conversion methods (e.g., slow pyrolysis), isocyanic acid and hydrogen cyanide were not detected in this study. The second stage produced activated biochar with a specific surface area of up to 865 m^2/g at 950°C. The volatile gases generated during activation were predominantly composed of toluene and benzene. This two-step process resulted in nitrogen-rich carbon in the form of pyrrolic and pyridinic nitrogen. Activated biochars were then evaluated for their SO_2 retention performance and showed an excellent adsorption capacity of up to 2140 mg/g compared to 65 mg/g for a commercial activated carbon (889 m^2/g). End-of-life reconstituted wood panels and SO_2 gas are problematic issues in Canada where the economy largely revolves around forestry and mining industries.

KEYWORDS

End-of-life wood panels; pyrolysis; activation; biochar and activated biochar; N-doped carbons; SO_2 removal

1 Introduction

According to a recent report on the recovery and recycling of materials in Canada, around 1.3 million tonnes of wood waste from construction, renovation, and demolition (CRD) are generated annually. This wood waste is classified as: (i) clean wood, suitable for several uses (49%; 637,000); (ii) engineered wood, a class of building products and materials such as mass timber, composite wood, man-made wood,

or manufactured board (23%; 299,000); (iii) painted wood (20%; 260,000); and (iv) wood treated with preservatives and other chemicals (8%; 105,300) [1]. A significant amount of low-grade wood waste is composed of veneers, flakes, particles, and wood fibers that are usually combined with thermosetting resins (e.g., urea-formaldehyde, melamine-formaldehyde, phenol-formaldehyde, and isocyanate) [2], which are rich in nitrogen such as aminoplast and various other chemical additives (e.g., kerosene wax, ammonium phosphate, zinc borate) [3].

Improper management of this type of waste can lead to serious health threats due to fires, explosions, and the contamination of air, soil, and groundwater [4]. The Canadian emissions reduction plan established new measures (e.g., varying the energy mix—coal, oil, gas, nuclear, hydropower, solar, wind, and biofuels) to remove excess carbon from the air and reach an emissions reduction of between 40% and 45% by 2030 [5]. Currently, a huge amount of CRD waste (low-quality wood) is deposited in Northern Québec's local sorting centers. Eventually, these materials are milled and transported to other centers, more than 400 km away, where they are incinerated. The carbon footprint of these activities is huge. Moreover, it is too expensive to ship all this wood waste for incineration, so it becomes an environmental issue and a health hazard given its leachable and toxic nature.

The main energy recovery of reconstituted wood panel waste is incineration, rather than recycling. Incineration relies on burning the waste to reduce its mass (70% to 80%) and volume (90%) while recovering thermal energy [6,7]. However, this practice negatively affects the quality of the environment, damages human health, and causes discomfort to the surrounding populations [8]. Incineration does not completely remove the waste or the contaminated residues and produces many toxic pollutants, such as bottom ash [9]. Furthermore, the combustion of wood waste containing aminoplast resins results in air pollution via the production of toxic pollutant gases such as ammonia, isocyanate, hydrocyanic acid, carbon monoxide, hydrocarbons, dioxins, hydrogen chloride, and nitrogen oxide [4]. NO_x is one of the gases of greatest concern for air quality, contributing significantly to the greenhouse effect and climate change [10].

Several wood decontamination approaches have been investigated at the laboratory scale, including electrodialysis [11,12], biological decontamination with bacterial cultures [13,14], chemical decontamination [15,16], and thermal decontamination, particularly pyrolysis [17–21]. The latter refers to biomass heating from moderate to high temperatures in the absence of oxygen. The advantage of this process is that the biomass is converted to a mixture of high-value-added bioproducts: biochar (solid), gas, and bio-oil (liquid). The pyro-gasification conditions (including temperature, residence time, heating rate, and reactor design) as well as the biomass feedstock strongly influence the properties of the resultant bioproducts [22].

Rybiński et al. [23] studied the incineration of wood (residues, pellets) and wood-based materials (furniture board, plywood) and quantified the associated toxic compounds and greenhouse gases. They noticed that the combustion of wood panels under controlled conditions could lead to emissions of toxic wastes equally as low as the combustion of traditional wood materials. However, Puettmann et al. [24] demonstrated that pyrolysis of forest residues to produce biochar reduced the global warming potential (GWP) of biochar by 1.9−2.8 tonne CO_2eq./tonne, compared to their combustion. Overall, the net GWP in biochar produced (0.1−1.6 tonne CO_2eq./tonne of residues) from forest residues can reduce the environmental impacts from twofold to fortyfold net CO_2eq. emissions, compared to their burning. Also, according to a life cycle analysis, pyrolysis of municipal solid waste recovered higher amounts of energy and reduced emissions of harmful gases, such as NO_x and SO_2, compared to combustion [25]. For example, a similar study by Hu et al. [26] on oily sludge indicated that pyrolysis achieved only 7% of the ecotoxicity impact of combustion, resulting in lower adverse effects on soil and groundwater. The normalized life cycle environmental impacts also indicated that pyrolysis recorded the lowest normalized

total value (47 impacts per person per year), followed by landfilling (586 impacts per person per year) and combustion (701 impacts per person per year).

The development of new synthesis routes with biomass as the carbon precursor has emerged as an environmentally friendly and economical alternative. Recently, increasing attention has been paid to synthetic methods to dope heteroatoms (nitrogen, bore, sulfur, phosphor, etc.) into carbon matrices to improve the physicochemical and electrocatalytic properties of carbon materials [27]. Due to their impressive electrocatalytic properties, nitrogen(N)-doped carbons have even been considered among the potential substitutes for platinum(Pt)-based electrocatalysts for oxygen reduction reactions, an essential reaction for energy conversion in fuel cells [27]. After thermal treatment, the proportion of nitrogen could be fixed into the carbon layer in three different forms: (i) pyridinic-N, bonded with two C atoms (hexagon form), (ii) pyrrolic-N bonded with two C atoms (pentagon form), and (iii) graphitic-N, which is bonded with three C atoms [28]. However, there are still many doubts and controversies concerning the optimal proportion of functionalized groups (e.g., nitrogenated and oxygenated, carboxylic, carbonyl and quinone) and textural characteristics, such as pore size and surface area, required for a specific application.

The traditional methods that produce N-doped carbons are dangerous and more suitable for laboratory-scale experiments. Normally, they are synthesized using an NH_3 treatment of the carbon material at high temperatures [29], chemical vapor deposition [30,31], or the pyrolysis of C–N containing compounds (e.g., urea-formaldehyde, polypyrrole, and dicyandiamide) [32,33]. Converting reconstituted wood waste (loaded with nitrogen compounds) into nitrogen-enriched carbon will avoid the need for complex and expensive nitrogen-doping chemical reactants, processes, and surface modification steps. N-doped carbons have been recently demonstrated to be great materials for electrochemistry [27,34], but also in treating water and air contaminants [35–37].

SO_2 is the main atmospheric contaminant released by industrial activities. This gas is mainly generated by the combustion of fossil fuels used to generate electricity and smelt ores. SO_2 produced by industry may cause acid rain, which contributes to air pollution, soil acidification, water pollution, and the destruction of building structures [38]. Adsorption of SO_2 by carbonaceous materials, particularly activated carbon, has been considered the most promising choice for the next generation of SO_2 removal technologies due to the advantages of water savings, low cost, and the ability to recycle the adsorbents [39]. Also, the advantage of N-doped carbons is that they present pyridinic and pyrrolic types of nitrogen which increase basicity to medium and enhance the capture of acid gases [40–42].

Thus, this project will offer an efficient and simple solution for the decontamination and revalorization of reconstituted wood waste to treat other kinds of wastes generated from forestry and mining exploitation in Canada. The effectiveness of naturally nitrogen-enriched carbon will be investigated for environmental applications—namely, removing pollutant gases such as SO_2, especially from mining and smelting activities. For sorting centers and CRD companies, the conversion of wood waste into high-value-added carbon materials with high potential for industrial applications is a path toward a regional circular economy.

2 Materials and Methods

2.1 Reconstituted Wood Panel Sample Preparation

Reconstituted wood panel wastes, usually combined with formaldehyde-based and nitrogen-rich thermosetting resins (aminoplast), were collected at the Val-d'Or Ecocenter (Enviroparc of the La Vallée-de-L'Or MRC) in the Abitibi-Témiscamingue region of Québec, Canada. Samples were coated with a layer of melamine but the proportion of wood and aminoplast resins was not precisely known. According to Girods et al. [43], the weight percentage of each component is about 88%–90% wood, 10%–12% urea-formaldehyde (UF) resin and less than 0.5% melamine-formaldehyde (MF) resin. Samples (uncoated particleboard and melamine coated sheets) were also collected at Teknion Corporation (Toronto, Canada),

a Canadian company specializing in the design and manufacture of office furniture (Fig. 1). Melamine coated sheets are typically used as decorative papers glued to wood-based panels for aesthetic reasons and to protect them from moisture. Also, balsam fir wood, an easily available wood species in the Abitibi-Témiscamingue region, was used for comparison purposes. All samples were ground with a rotary cutter mill (Thomas-Wiley, model 4, Swedesboro, USA) using a 2 mm sieve size.

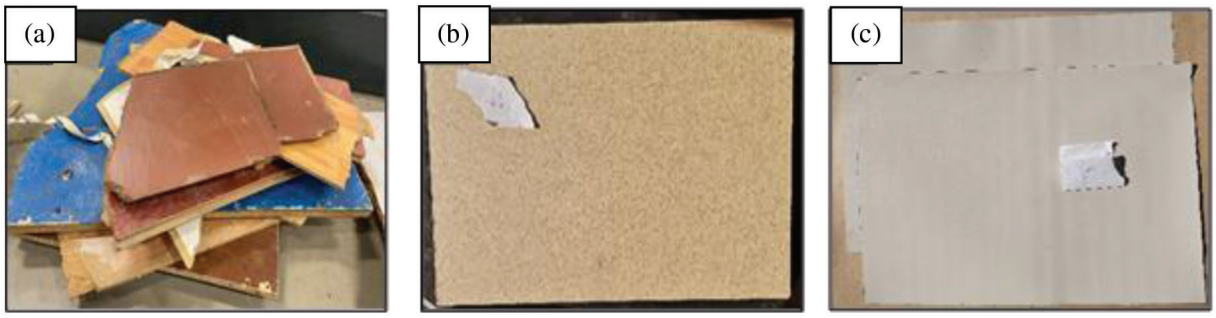

Figure 1: The different wood panel samples: (a) Wood-based panel waste; (b) Uncoated particleboard; and (c) Melamine coated sheets

2.2 Biochar Pyrolysis and Activation

The particle panels (54 kg) were first ground using a hammer mill equipped with a 12 mm grate and an aspirator (Schutte-Buffalo Hammer mill, model 1320, Buffalo, New York, USA). Fast pyrolysis was carried out using CarbonFX technology (Airex Energy Inc., Bécancour, QC, Canada). Wood panels were converted to biochar at 450°C for 2 s in a cyclonic fluidized bed reactor (250 kg/h) in a low oxygen atmosphere environment. After pyrolysis, the resulting biochar was fed into an in-house activation furnace developed in the laboratory, for physical activation. Biochar was converted into activated biochar at 750°C, 850°C, and 950°C under a constant CO_2 and N_2 flow rate of 3 L/min. More details about these processes can be found elsewhere [44]. The synthesized biochar and activated biochars were designated as BWP, and BWP750, BWP850, and BWP950, respectively.

2.3 Physicochemical Characterization

2.3.1 Elemental Composition

Elemental analyses to determine the percentages of carbon (C), hydrogen (H), nitrogen (N), and sulfur (S) of particleboard waste, uncoated particleboard, melamine coated sheets, fir wood, biochar, and activated biochars were performed by a CHNS Analyzer (Perkin Elmer 2400 Series II, Waltham, Massachusetts, USA). These analyses were carried out to evaluate the efficiency of the nitrogen removal processes. The level of nitrogen devolatilization was deduced from the results of the elemental analyses and their degradation level after thermal treatment according to Eq. (1):

$$N_{removed} = \frac{N_i * m_i - N_f * m_f}{N_i * m_i} * 100 \quad (1)$$

where $N_{removed}$: Mass percentage of nitrogen removed during each thermal treatment test; N_i: Nitrogen content in the sample before thermal treatment; m_i: Initial mass of each sample before thermal treatment; N_f: Percentage of nitrogen in each sample after thermal treatment; m_f: Residual mass of each sample after thermal treatment.

2.3.2 Thermogravimetric Analysis (TGA) Coupled with Gas Chromatography-Mass Spectrometry (GC/MS)

The thermal stability and degradation behavior of particleboard samples were analyzed using a Jupiter Netzsch STA 449 F5 thermogravimetric analyzer (Exton, PA, USA). In each experiment, a fixed amount of sample was placed in a ceramic cup on a microbalance and the temperature was increased from 35°C to 450°C at 20 °C/min. Helium was maintained at 50 mL/min to keep the atmosphere inert. However, the pilot scale CarbonFX could not provide a completely inert medium and 5 mL/min of pure oxygen was thus added to achieve a system that was as close as possible to the CarbonFX process.

The gases released during the thermal treatment of particleboard at 450°C were transported from the TGA to the GC/MS (Agilent Technologies 789B, Santa Clara, California, USA), whereas the gases produced during activation were recovered with gas bags and manually injected with a syringe into the GC/MS system. The gases generated during the thermal treatment in the Netzsch analyzer were transported through an He carrier gas (1 mL/min) to the chromatography HP-5 type capillary column (30 m × 0.25 mm × 0.25 µm). The volume injected into the column was 1 µl at 100°C every minute, i.e., every 20°C increase. The identification of the gas compounds released during the TGA or during the activation in the in-house furnace was carried through the NIST02 spectra library. Blank GC/MS tests were performed before each test to ensure that the GC column was purged.

2.3.3 Surface Chemistry Analysis by X-ray Photoelectron Spectroscopy

X-ray photoelectron spectroscopy (XPS) using a Kratos Axis Ultra DLD spectrometer (Manchester, UK) equipped with Al anode ($h\nu = 1486.6$ eV) and operated at 225 Watts was used to analyze the wood panel waste, biochar and activated biochars. The spectrum was recorded with a pass energy of 80 eV, and a step size of 1 eV. Atomic concentrations were obtained by the integration of each elemental peak. A scan from 0 to 1400 eV was acquired and the elemental composition of the surface of each sample was calculated using CasaXPS software.

2.3.4 Measurement of Specific Surface Area and Pore Distribution

The specific surface area (S_{BET}) and pore size distribution were performed using a high-resolution physical surface analyzer (Micromeritics ASAP 2460, Norcross, Georgia, USA). The biochar and activated biochars were degassed at 105°C and 250°C, respectively, under vacuum for 48 h. Nitrogen and carbon dioxide were used as adsorbates at −196°C and 0°C, respectively. The isotherms obtained from the N_2 adsorption tests were processed using the Brunauer-Emmett-Teller (BET) method to determine: (i) S_{BET} [45]; (ii) micropore volume (V_μ, cm^3/g) according to the Dubinin-Radushkevich method [46]; (iii) total pore volume (V_t, cm^3/g) calculated at the relative pressure of 0.97 from the amount of nitrogen adsorbed [47]; (iv) mesopore volume (V_m, cm^3/g) calculated by the difference $V_t - V_\mu$; and (v) pore size distribution by applying density functional theory to N_2 adsorption isotherms [48].

2.4 SO_2 Adsorption Tests

Dynamic tests were performed at room temperature to evaluate the ability of the biochar and activated biochars to adsorb SO_2. The breakthrough capacity of SO_2 adsorption was measured according to the American standard test [49] using the adsorption test device shown in Fig. 2. The samples (1.5 g) were placed in a 27 cm long and 2.5 cm diameter glass column. The SO_2 concentration at the column inlet was maintained at 150 ppm at 30 mL/min by mixing 10,000 ppm of standard SO_2 with air using a flowmeter. The outlet SO_2 concentration was measured using a GazBadge®Pro gas detector (Industrial Scientific, Pittsburgh, USA) and the test was stopped when the outlet concentration was equal to the inlet concentration. The SO_2 removal efficiency was calculated by Eq. (2):

$$SO_{2\ removal\ efficiency}\ (\%) = \frac{C_{\mathrm{i}} - C_f}{C_{\mathrm{i}}} * 100 \tag{2}$$

where C_i: SO_2 concentration at the inlet; and C_f: SO_2 concentration at the outlet.

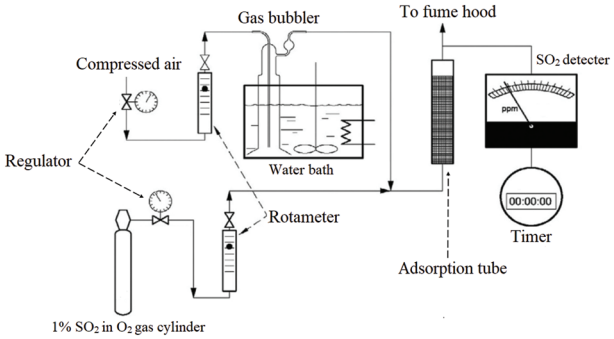

Figure 2: The SO_2 adsorption device used in this study

The SO_2 saturation capacities (Q) of all materials were calculated by integrating the area above the saturation curves and the saturation time [Eq. (3)]. For each sample, saturation tests were repeated at least five times to ensure that the textural properties and SO_2 adsorption capacities of the activated biochars prepared in pilot furnaces were reproducible.

$$Q = \frac{F \int_0^t (C_i - C_f) dt}{m} \tag{3}$$

where Q: SO_2 saturation capacity of materials (mg/g); F: SO_2 flow rate (L/min); C_i: SO_2 concentration at the inlet (ppm); C_f: SO_2 concentration at the outlet (ppm); and m: mass of each adsorbent (g).

3 Results and Discussion

3.1 Characterization of Reconstituted Wood Panels, Biochars and Activated Biochars

3.1.1 Thermogravimetric Analysis

To study the thermal behavior of samples, the thermogravimetric (TG) curves and their derivatives (DTG) for particleboard and fir wood (control) are presented in Fig. 3. The TG analyses were performed using a temperature range between 35°C and 450°C at 20°C/min. The pyrolysis process can be divided into three stages for both samples. For the first stage, the mass loss occurred between 35°C and 200°C, i.e., 8% and 2% for wood and particleboard, respectively, due to the evaporation of water and volatile compounds. The second stage, between 200°C and 400°C, is where cellulose, hemicellulose, lignin, urea-formaldehyde (UF), and melamine-formaldehyde (MF) resins were thermally degraded. The mass loss at this stage was about 54% and 58% for wood and particleboard samples, respectively.

The particleboard reached its highest degradation rate of 14% at 356°C, while fir wood reached 19% at 366°C. This indicates that UF and MF resins accelerate the chemical reactions causing particle board degradation, which is in agreement with results reported by Feng et al. [6]. The third stage, between 400°C and 450°C, is when only lignin continues to pyrolyze. The TG curve also shows that the final mass of the pyrolyzed samples was about 29% and 32% for wood and particleboard, respectively. Moreno et al. [50] stated that the degradation temperature range for particleboard is close to that of wood, as particleboard contains approximately 90% wood. However, there is a slight difference in the appearance of a peak at 308°C due to the decomposition of urea-formaldehyde (UF) resin [51]. The

results of the thermogravimetric analysis show that the highest degradation rate for particleboard is 356°C. Indeed, the pyrolysis process of particleboard from this study was performed using CarbonFX technology at 450°C for 2 s. The choice of such a temperature was to avoid any kind of tar formation during the production of the activated biochar in the in-house activation furnace.

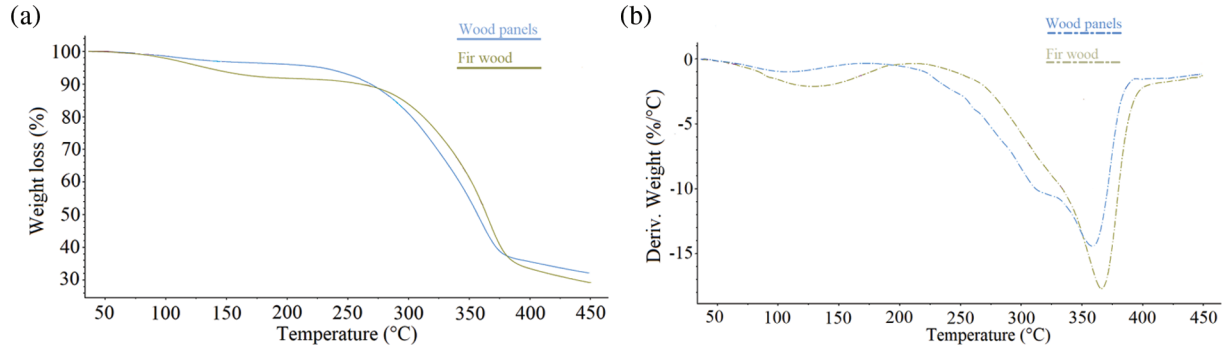

Figure 3: (a) TG mass degradation curves and (b) their derivatives (DTG) for fir wood (green) and particleboard (blue) samples

3.1.2 Elemental Composition

Elemental analyses performed on wood panels and their components separately, and on biochar and activated biochars are summarized in Table 1. Specifically, nitrogen was present in all samples, but at a higher percentage compared to fir wood (>2.45% *vs.* 0.13%). The high nitrogen content is explained by the presence of urea-formaldehyde glue and melamine-formaldehyde coating as shown by Girods et al. [43]. This result is consistent with Feng et al. [20] who reported content of 7.4% nitrogen in the particleboard. This difference is probably due to the varying percentages and types of glue used in the panels. However, the nitrogen content present in BW, BWP and activated BWP decreased from 4.29% to 2.45% (BWP950). Indeed, the resins associated with wood degrade at a lower temperature range compared to fir wood, resulting in the removal of a greater amount of resin initially present in the wood panels. This statement is in agreement with other studies from the available literature [50,52,53].

Table 1: Elemental analysis of fir wood, wood panels and their respective biochar and activated biochars

		C (%)	H (%)	N (%)	S (%)
Wood panels (WP) and fir wood in their raw state					
Fir wood		46.84 ± 0.4	6.32 ± 0.17	0.13 ± 0.05	0.97 ± 0.05
WP	Panel, no coating	49.26 ± 3.62	6.68 ± 0.40	4.53 ± 0.51	0.80 ± 0.05
	Melamine coating	32.23 ± 0.54	5.20 ± 0.08	22.67 ± 0.61	0.66 ± 0.07
WP		45.8 ± 0.02	6.23 ± 0.02	4.29 ± 0.05	1.41 ± 0.04
Biochar prepared at 450°C					
BWP	Panel, no coating	41.73 ± 1.20	2.49 ± 0.14	17.77 ± 0.39	0.27 ± 0.07
	Melamine coating	77.50 ± 0.24	3.89 ± 0.03	4.07 ± 0.24	0.42 ± 0.05
BWP		69.17 ± 0.11	3.23 ± 0.09	3.32 ± 0.01	0.87 ± 0.10

(Continued)

Table 1 (continued)

	C (%)	H (%)	N (%)	S (%)
Activated biochars prepared at 750, 850 and 950°C				
BWP750	78.99 ± 1.25	1.85 ± 0.12	3.82 ± 0.15	1.83 ± 0.21
BWP850	79.38 ± 2.02	1.57 ± 0.03	3.03 ± 0.16	1.62 ± 0.10
BWP950	81.18 ± 1.06	1.46 ± 0.20	2.45 ± 0.23	1.47 ± 0.14

After pyrolysis, the carbon content of the biochar and activated biochars increased and the hydrogen content decreased compared to their precursors. This is due to the release of volatiles during pyrolysis which results in the removal of non-carbon species and promotes carbon enrichment [54]. Thus, the activation step was responsible for an increased carbon content from 69.17% to 81.18%, while the percentage of hydrogen decreased from 3.23% (BWP) to 1.46% (BWP950). The results also revealed that the percentages of C and H slightly increased and decreased, respectively, with an increase in the activation temperature from 750°C to 950°C (78.99% and 1.85% *vs.* 81.18% and 1.46%). This is due to the progressive consumption of carbon and hydrogen atoms by the CO_2 gas during physical activation and by the simultaneous formation of oxygenated sites on the walls of the activated carbon [55]. Nitrogen was present in all activated carbon samples, ranging from 2.45% to 3.82%. The two-step thermochemical treatment, fast pyrolysis followed by physical activation in the presence of CO_2, allowed the activated biochars to acquire a stable amount of nitrogen content. According to the literature, activated biochars prepared from wood panels have an excellent adsorption capacity for acid gases and phenolic compounds due to their nitrogen-containing surface groups [19]. To evaluate the efficiency of the thermal treatment, the percentage of nitrogen removed during the pyrolysis of different samples was calculated from the results of the elemental analyses and the residual mass. The results showed that approximately 66% of nitrogen initially present in the different panel components was removed during the pyrolysis process. Furthermore, the efficiency of the process in terms of nitrogen removal does not appear to be influenced by the percentage of nitrogen initially present in the samples.

The percentages of nitrogen removed by the pyrolysis treatment in this study are in agreement with those reported in the literature [17–18,43,51,53]. Girods et al. [17] reported that an appropriate pyrolysis temperature (250°C–300°C) and residence time (8–15 min) could effectively remove about 70% of the initial nitrogen content in wood panels. Lemonon et al. [53] showed that the nitrogen removal efficiency was about 66% for the pyrolysis of melamine flooring at a temperature of 275°C and a residence time of 11 min. In another study, Zhan et al. [56] demonstrated that proper pyrolysis at low temperatures (250°C–300°C) could effectively achieve 63% nitrogen removal from medium-density fiberboard (MDF). In the present study, the fast pyrolysis process at 450°C for 2 s was also efficient for nitrogen removal. As previously mentioned, 450°C was chosen to avoid tar formation during biochar activation in the continuous in-house activation furnace. In addition, fast pyrolysis using the CarbonFX technology (250 kg/h) is a pilot scale process compared to laboratory scale furnaces (few grams in a static furnace) used in the studies mentioned above.

3.1.3 Specific Surface Area and Pore Distribution

Textural characteristics such as specific surface area and pore size distribution of biochar and activated biochars are presented in Table 2. The N_2 adsorption and desorption isotherms of activated biochars pyrolyzed at 450°C and activated at 750°C, 850°C and 950°C are presented in Fig. 4. According to the

International Union of Applied Chemistry (IUPAC) classification, the isotherms obtained for the BWP750 and BWP850 are of type I, which reflects the presence of micropores of 2 nm or less. On the other hand, the isotherm obtained for the activated biochar at 950°C belongs to types I and IV, which indicates that the activated biochar produced contains a mixture of micropores and mesopores. As expected, the use of CO_2 as an activating agent during physical activation mainly produces microporosity in the carbon material [57]. All three activated carbons are predominantly microporous at proportions of 85%, 78%, and 66% for the activated biochars prepared at 750°C, 850°C, and 950°C, respectively (the remaining being mesopores).

Table 2: Textural properties of biochar and activated biochars derived from particleboard pyrolyzed at 450°C and activated at 750°C, 850°C and 950°C

	S_{BET} (m^2/g)	V_μ (cm^3/g)	V_m (cm^3/g)	V_t (cm^3/g)
BWP	99 ± 4	–	–	–
BWP750	450 ± 8	0.156 ± 0.003	0.028 ± 0.0004	0.183 ± 0.003
BWP850	682 ± 36	0.227 ± 0.013	0.066 ± 0.066	0.293 ± 0.014
BWP950	866 ± 46	0.272 ± 0.014	0.139 ± 0.007	0.411 ± 0.020

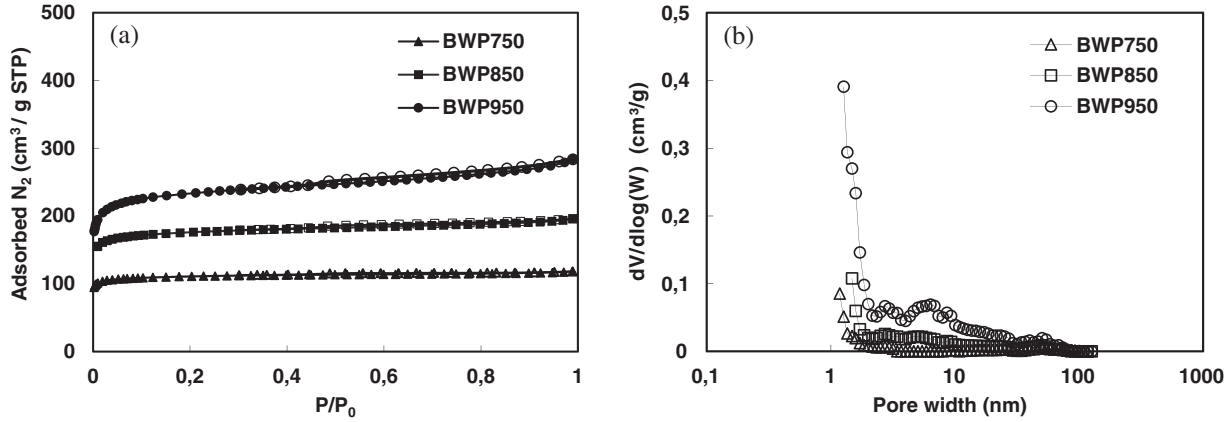

Figure 4: (a) N_2 adsorption–desorption isotherms (full and open symbols, respectively) at −196°C; and (b) PSD determined by the DFT method and N_2 isotherms for activated biochars: BWP750, BWP850 and BWP950

Nitrogen adsorption isotherms were used to determine the specific surface area, micropore, mesopore, and total pore volume of the different activated biochars, as seen in Fig. 4. The biochar developed low porosity due to the low pyrolysis temperature (450°C) and short residence time (approximately 2 s) in the CarbonFX fast pyrolysis reactor [44]. In addition, attempts to use N_2 gas for biochar adsorption analysis were unsuccessful, as biochar is generally very microporous, with ultramicropores (smaller than 0.7 nm). These limitations in ultramicroporosity analysis using N_2 are due to diffusion restrictions at low pressure, which prevent nitrogen from entering the narrowest micropores. The use of CO_2, rather than N_2 (−196°C), for adsorption analysis is suggested when the analysis is performed at moderate pressures and higher temperatures (0°C) [58].

The specific surface area of biochar derived from pyrolyzed particleboard at 450°C was 99 m^2/g. However, the activated biochars had much larger specific surface areas, ranging from 450 to 866 m^2/g. It can also be seen that the micropore, mesopore, and total pore volume increased with increasing temperatures from 0.155 to 0.272 cm^3/g, 0.028 to 0.139 cm^3/g, and 0.183 to 0.411 cm^3/g, respectively. This increase in pore volume and specific surface area is due to the penetration of an oxidizing agent (CO_2) into the internal structure of the biochar, thereby resulting in the removal of carbon atoms, and consequently, the opening and widening of inaccessible pores [59]. Among all the activated biochars obtained, the biochar activated at the highest temperature (950°C) had the highest specific surface area, micropore, mesopore and total pore volume, 866, 0.272, 0.139 and 0.411 cm^3/g, respectively. A study of the pyrolysis of particleboard waste carried out using a laboratory-scale quartz tube reactor at 250°C, 300°C, and 400°C, followed by activation in the presence of steam at 800°C, 900°C, and 1000°C, presented specific surface areas between 800 and 1300 m^2/g and pore volumes between 0.37 and 0.73 cm^3/g [19]. Thus, the results from the present study using a larger scale are closer to the ones presented in the literature (at laboratory scale).

3.1.4 Surface Chemistry Analysis by X-ray Photoelectron Spectroscopy

XPS analysis was performed to obtain a clear understanding of the nitrogen functionalities in the different samples as well as to study the chemical changes that occur in the biochar and activated biochars prepared by pyrolysis and further activation, respectively. By identifying the energies associated with each peak, it was possible to determine the nature of the chemical elements present in these materials. Carbon (C 1s, 284 eV), oxygen (O 1s, 532 eV) and nitrogen (N 1s, 400 eV) were clearly identified in all spectra. Relatively weak peaks of other elements such as sulfur (S 2p), sodium (Na 1s) and calcium (Ca 2p) were also observed. The integration of the area of each peak after the removal of the baseline (Appendix, Fig. S1) allowed the determination of the atomic concentration of the different elements which are summarized in Table 3.

Table 3: Contributions to the N1s bands in XPS patterns and the atomic content of wood panels, biochar and activated biochars

	Area of the peak (%)			Atomic content (%at.)			
	N-5 (399.9–400.9 eV)	N-6 (398.6–398.8 eV)	N-X (402.1–402.6 eV)	C	O	N	S
WP	94.1	0	5.9	74.9	21.1	3.4	-
BWP	68.2	27.3	4.5	82.2	14.7	2.2	0.2
BWP750	50	41.7	8.3	91.7	5.2	2.4	0.1
BWP850	53.8	38.5	7.7	94	4.1	1.3	0.1
BWP950	57.1	28.6	14.3	93.5	4	1.4	0.2

The elemental composition obtained by XPS is different from the one obtained by elemental analysis. This means that the elemental composition at the surface of the material is different from that within the sample. This is because the distribution of surface functional groups in the sample is not uniform [60]. This difference between the elemental composition obtained by XPS and that obtained by elemental analysis was also observed by Xu et al. [61] on biochar derived from fiberboard. The carbon percentage is always higher when measured by XPS, while the nitrogen percentage is always lower. Despite this, the

trend of increasing carbon percentage and decreasing nitrogen percentage after pyrolysis and activation is the same as that observed for elemental analysis. The carbon percentage of the particleboard increased from 74.9% to 82.2% after pyrolysis and 93.5% after activation performed at 950°C. While the percentage of nitrogen decreased from 3.4% to 2.2% and 1.4%, respectively. The N 1s peak of each sample was deconvoluted to identify and estimate the relative proportions of the nitrogenous functional groups. The deconvoluted XPS N 1s spectra of the particleboard, biochar, and activated biochars, and the relative contributions of each nitrogen species are also presented in Fig. S2 (Appendix) and Table 3. The peaks can be attributed to pyridine nitrogen (N-6, 398.7 ± 0.3 eV), pyrrole nitrogen (N-5, 400.3 ± 0.3 eV), and nitrogen oxides (N-X, 402–405 eV) [52]. The dominant nitrogen species in the particle panel, biochar, and activated biochars were N-5, N-6 and N-X, respectively. These results are in good agreement with the activated biochars derived from medium density fiberboard reported by Wu et al. [62]. N-5 accounted for 94.1% of the nitrogenated species in the particleboard (5.9% N-X), but after activation, N-6 appeared and N-5 was reduced for all samples. These results reveal that the chemical state of nitrogen sensitively changed after the thermochemical treatments.

3.1.5 Analysis of the Gases Emitted during the Pyrolysis of Particleboard and Activation

To obtain information on the release of volatile organic compounds during the pyrolysis of particleboard, a thermal degradation process was performed by TGA coupled with GC/MS gas analysis. The sample was studied in quasi-continuous mode, i.e., the evolved gas was ejected every minute into the GC at 100°C. The peaks were characterized and a total of 11 compounds were identified: methane, nitric oxide, trimethylamine, ammonia, carbon dioxide, 1,1-dimethylhydrazine, acetic acid, methylamine, 8-hydroxy-2-octanone, 1-propanol, and 5-hydroxy-2-pentanone. Based on the areas under the chromatographic peaks associated with the different compounds, CO_2 was the major compound emitted during pyrolysis and was detected at temperatures above 250°C. The formation of CO_2 can be mainly attributed to the cracking and rearrangement reactions of carbonyl and carboxyl groups in organic compounds and to the decomposition of carbonates from inorganic compounds [63]. Indeed, during pyrolysis, hemicellulose and cellulose are converted to carbonyls by cracking, while lignin is converted to phenols by dehydration, depolymerization, and decarboxylation [21]. In addition, CH_4 was emitted at low temperatures from 56°C to 156°C due to the cracking of methoxy, methyl, and methylene groups [64].

The analysis of mass spectroscopy data revealed the release of several nitrogenous compounds during pyrolysis, mainly nitric oxide, ammonia, and trimethylamine, which were observed in the temperature ranges of 176°C–255°C, 239°C–301°C, and 287°C–385°C, respectively. These nitrogenous compounds were produced by the degradation of their main precursors, urea-formaldehyde and melamine-formaldehyde [53]. Indeed, nitrogenous gases from the pyrolysis of wood-based panels are significantly influenced by the addition of UF and MF resin [65]. These results are in agreement with the available literature given that most of the compounds were already identified by Girods [66] and Moreno et al. [50]. However, Feng et al. [6] identified isocyanic acid (HNCO) and hydrogen cyanide (HCN) during the pyrolysis of particleboard at 800°C with a heating rate of 20 °C/min using a thermogravimetric analyzer coupled with Fourier transform infrared analysis (TG-FTIR). Neither compound was identified in this study. The composition of the pyrolytic gas depends on several factors such as the pyrolysis reactor, temperature, residence time, heating rate and feedstock [21]. The present study is only based on the fast pyrolysis of particleboard at a pilot scale, while the studies available in the literature used slow pyrolysis furnaces at a laboratory scale.

A semi-qualitative analysis of the gases emitted during the activation of the particleboard-derived biochar was performed using a GC/MS analyzer to identify the volatile organic compounds emitted at 750°C, 850°C, and 950°C. A condenser was used to condense the gases. A sample was taken before and after condensation to evaluate the efficiency of the condenser. The analyzed gases were recovered through the activation process using gas bags. The main gases generated during activation before and after condensation were nitric oxide, ethylenediamine, carbonyl sulfide, benzene, toluene, p-Xylene, styrene,

1,3-cyclopentadiene, acetylene, hydrogen sulfide and acetic acid. The emissions resulting from the activation of particleboard biochars were dominated by aromatic hydrocarbons and, in particular, toluene and benzene, which were detected at the three different activation temperatures. While other aromatic hydrocarbons, such as p-Xylene and styrene, were detected at very low concentrations. The emission of two nitrogen species was also noted for all gas samples, including nitric oxide and ethylenediamine, probably due to the decomposition of pyridinic-N, pyrrolic-N and nitrogen oxides present in the biochar. Also, two sulfur compounds were released during activation given that the percentage of sulfur present in biochar was 0.87%, namely carbonyl sulfide (COS) which is present in all samples and hydrogen sulfide (H_2S) detected only at 850°C after gas condensation. The gases released before and after condensation were almost the same.

3.2 Study of the Potential of Biochar-Based Material for the Adsorption of SO_2

In this study, SO_2 adsorption by the biochar and activated biochars derived from particleboard was investigated. To ensure the robustness of the experimental data, SO_2 adsorption tests at a concentration of 150 ppm and an inlet flow rate of 30 mL/min were repeated at least three times for the four-biochar based-materials and for a commercial activated carbon (CAC), Darco G-60 100-Mesh, used as a control. SO_2 adsorption behavior exhibited by these porous solid sorbents is shown in Fig. 5. The SO_2 adsorption capacity and breakthrough time for all samples are summarized in Table 4. According to the results, the activated biochar at 950°C was the most efficient adsorbent for SO_2 (150 ppm) removal, reaching up to 2138 mg of SO_2 per g of activated biochar. Furthermore, the activation temperature had an important impact on SO_2 adsorption. Indeed, adsorption capacity and time to saturation increased with increasing activation temperature and, consequently, the higher the specific surface area, the higher the adsorption capacity. Saturation of the carbon samples was reached after 2.3 h (150 mg/g) and increased to 3.4 (347 mg/g), 13.3 (1117 mg/g) and 19.4 h (2138 mg/g) after biochar activation at 750°C, 850°C and 950°C, respectively.

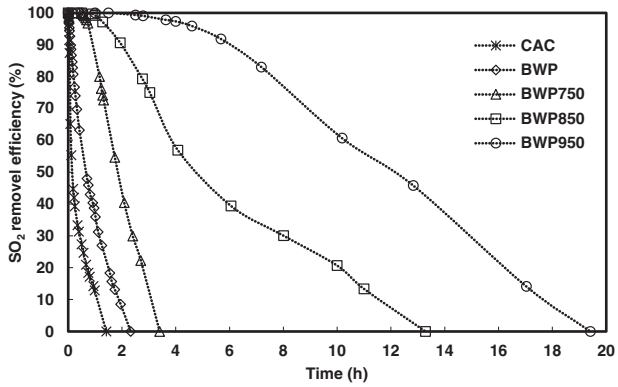

Figure 5: SO_2 removal efficiency curves as a function of saturation adsorption time for the commercial activated carbon (CAC), biochar (BWP) and activated biochars: BWP750, BWP850, and BWP950

Compared to results for other N-doped carbon materials in the available literature, the generated nitrogen-rich activated biochars had very high SO_2 adsorption capacities, despite the fact that the adsorption test conditions varied considerably (Table 5). This means the type of adsorption test (dynamic column apparatus, thermogravimetric analyser or fixed-bed experimental system), the amount of carbon material applied (0.1–25 g), SO_2 concentration (50–3000 ppm) and its flow rate (20–1500 mL/min), and the different kinds of N-doped carbons (e.g., ordered mesopores, carbon nanotubes). Wang et al. [67] developed an N-doped carbon material composed of 1.3% nitrogen (determined by XPS analysis), with a 1370 m^2/g specific surface area, 0.62 cm^3/g total pore volume and an SO_2 adsorption capacity of approximately 115 mg/g at 1200 ppm. The difference in SO_2 concentration between Wang et al. [67] and the present study (1200 ppm *vs.* 150 ppm) prevents us from comparing the two studies.

Table 4: SO_2 adsorption capacity of biochar, activated biochars, a commercial activated carbon (CAC)

Materials	Adsorption capacity (mg SO_2/g)	Breakthrough time (h)
BWP	150	2.3
BWP750	347	3.4
BWP850	1117	13.3
BWP950	2138	19.4
CAC (Darco G-60)	65	1.4

The plots of the amount of SO_2 adsorbed *vs.* the surface areas (Fig. 6a), pore volumes (Figs. 6b–6d) and nitrogen and oxygen contents of BWP750, BWP850, and BWP950 (Figs. 6e,6f) reveal linear relationships. However, there is an important difference between BWP and activated biochars made from wood residues from sawmills, as well as between BWP and commercial activated carbon (CAC). In a previous study, Braghiroli et al. [68] prepared activated biochars derived from wood residues (white birch) that were saturated with SO_2 after up to 1–1.4 h (activated biochars in the presence of CO_2 or steam). The biochar is made from wood residues saturated after approximately 20 min at 50 ppm. In this study, the same material rapidly saturated at 150 ppm in approximately 1 min. It is interesting that the biochar prepared from wood panels (BWP) reached an SO_2 adsorption capacity of 150 mg/g with a lower surface area (99 m^2/g) compared to the biochar made from white birch sawmill residues (177 m^2/g; 20.4 mg/g). The mechanism of SO_2 adsorption onto carbon materials is not well known due to the complex porous structure of carbon materials made from bio-precursors. What is known is that SO_2, O_2 (atmosphere) and H_2O (water vapor) will be first adsorbed onto the carbon material and SO_2 will then be oxidized into SO_3 and converted into H_2SO_4 [68]. The high SO_2 adsorption capacity observed for activated biochars made from wood panels could be explained by the presence of nitrogen in their composition, as nitrogen increases the alkalinity of the material and provides active sites for SO_2 adsorption [69]. As reported in the literature, nitrogen-containing functional groups can effectively contribute to the adsorption performance of biochar and activated biochars [40,62,70,71].

The activated biochars made from wood panels took an even longer time to saturate with SO_2 (ranging from 3.4 to 19.4 h). This can probably be explained by the difficult access of adsorbate to free sites in the pores. That is, the adsorbate must pass through the mesopores to reach the micropores where adsorption typically occurs, which explains the slow saturation of biochars after SO_2 detection begins [72]. When comparing our results with other kinds of materials and commercial activated carbons (Table 5), we can see that the percentage of nitrogen plays an important role in SO_2 adsorption capacity. For example, the commercial activated carbon Darco G-60 presents good textural properties (surface area and micropore, mesopore and total pore volumes of 889 m^2/g, 0.31, 0.34, and 0.65 cm^3/g, respectively), no nitrogen content, and its SO_2 adsorption reached 65 mg/g at 150 ppm [73]. Indeed, the activated biochar at 950°C also had good textural properties (866 m^2/g, 0.27, 0.14 and 0.41 cm^3/g, respectively), nitrogen contents of 1.4% (determined by XPS analysis) and 2.45% (determined by elemental analysis), and the highest SO_2 adsorption capacity (2138 mg/g) at the same concentration (150 ppm) among the prepared activated biochars. This difference in adsorption capacity is explained by the difference in nitrogen species and pore size distribution (micropores *vs.* mesopores proportion).

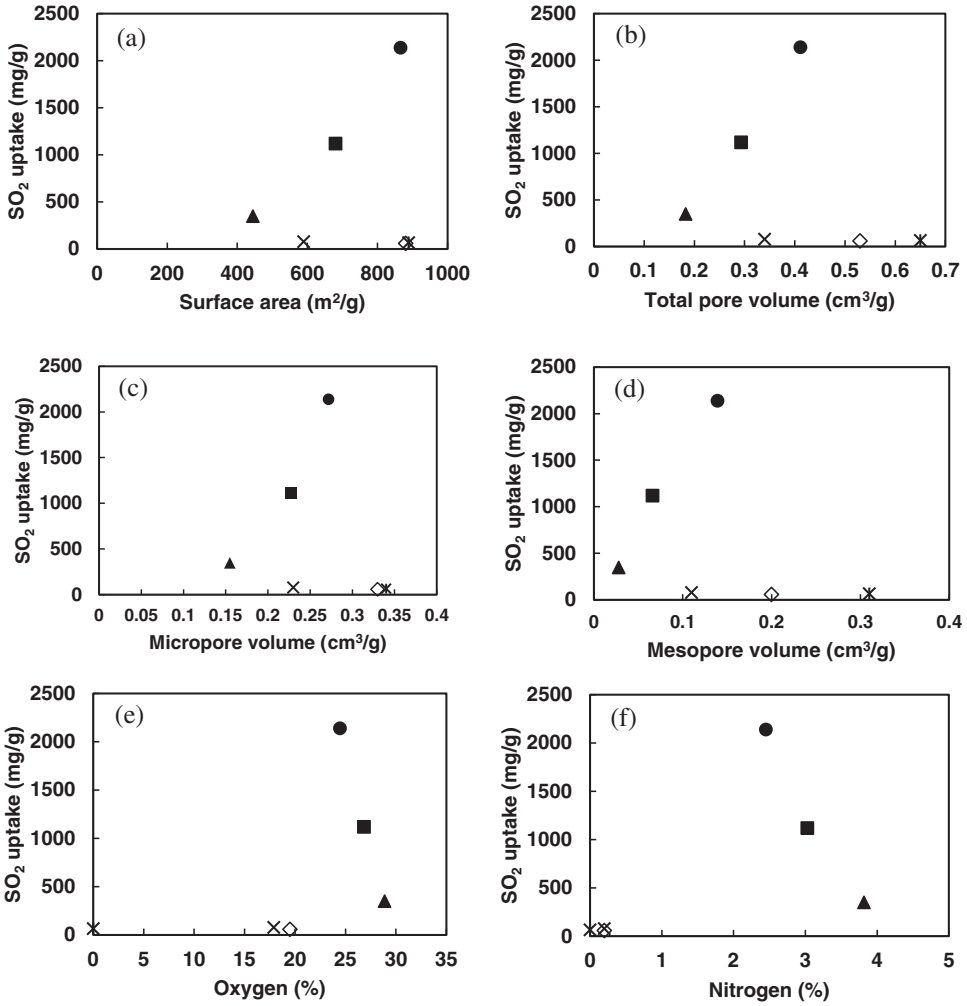

Figure 6: Relationship between SO_2 uptake and (a) surface area, (b) total pore, (c) micropore, and (d) mesopore volumes, (e) oxygen and (f) nitrogen contents of Darco G-60 (Ж), activated biochars made from particleboard waste: BWP750 (▲), BWP850 (■) and BWP950 (●), and activated biochars made from wood waste from sawmills in the presence of steam (◊) and CO_2 (x)

Indeed, some researchers have found that pyridine-N promotes SO_2 adsorption by enhancing the electrostatic interaction of adjacent carbon atoms and the van der Waals force between the surface of the carbon materials and SO_2 [39]. Also, the adsorption capacity of porous adsorbents generally depends on their specific surface area as there are more free sites for the adsorption process [74]. High micropore ratios are also favorable for SO_2 adsorption. Liu [75] showed that the adsorption capacity of SO_2 depends proportionally on the micropore ratio or pore size distribution, i.e., the higher the micropore ratio, the higher the adsorption capacity of SO_2. Also, the naturally nitrogen-doped activated biochars made from end-of-life wood panels may contain sulphur, anions (Cl) and metals that could be interesting for the efficient removal of various other gaseous pollutants (CO_2, NO, elemental mercury) [76,77]. Thus, the performance of activated biochars for the removal of other pollutant gases will be investigated in future work.

Table 5: Comparative SO_2 sorption capacity of carbon-derived materials

Material precursor	Thermochemical treatment conditions	S_{BET} (m^2/g)	SO_2 adsorption test conditions	SO_2 adsorption capacity (mg/g)	N (wt.%)	References
Activated biochar made from cork powder	Pyrolysis at 750°C and further activation in presence of KOH or CO_2 at 750°C	KOH: 584 CO_2: 76	Thermogravimetric analyser SO_2: 3300 ppm Flow rate: 120 mL/min	90 65	0.3 1.5	[78]
N-doped ordered mesoporous carbon spheres	Urea–phenol–formaldehyde resin and copolymer F127 (soft template) Carbonisation at 600°C for 3 h; Activation at 600°C in presence of KOH for 1 h	566	Dynamic test SO_2: 1800 ppm Flow rate: 80 mL/min	119	0.9	[79]
N-doped carbon	Copolymerization of phenol, NaOH, melamine, formaldehyde and tetraethyl orthosilicate (TEOS) Carbonisation at 900°C for 3 h	1013	Dynamic test Material: 0.1 g SO_2: 500 ppm Flow rate: 200 mL/min	48	10	[40]
Activated biochar made from corncobs	Pyrolysis at 600°C followed by activation in presence of CO_2 at 850°C and further impregnation with methyldiethanolamine	-	Fixed-bed experimental system at 120°C SO_2: 1% Flow rate: 20 mL/min	156	6.5 (at. %)	[80]
N-doped microporous carbon	Pyridine ligand-based metal–organic complexes (MOCs) Carbonization at 800°C–1100°C for 2 h	1656	Quartz reactor experimental system Material: 0.1 g SO_2: 2000 ppm	118	7.3	[81]
*CNH MWNT SWNT VACNT GO Norit: Activated carbon	CHN: Arc discharge of graphite in water SWNT, MWNT, Norit: Commercial GO: Graphite oxidized VACNT: Chemical vapor deposition	168 284 557 438 268 1375	Gravimetric setup with an automatic gas-dosing system SO_2: 3 bar	224 320 545 577 - 673	1.1 - 1.2 - - 0	[82]
N-doped porous carbon	Metal organic complex (MOC) carbonized at 900°C for 2 h	3187	Dynamic test Material: 5 g SO_2: 2000 ppm Flow rate: 1.5 L/min	157	20	[83]
Activated biochar made from wood residues	Fast pyrolysis (250 kg/h) at 454°C and further activation in presence of steam at 900°C	590	Dynamic test Material: 10–25 g SO_2: 50 ppm Flow rate: 30 mL/min	77	0.2	[68]
N-doped carbon: Anthracite, MgO, KOH and carbamide	Mixture stirred for 1 min through a high-speed pulverizer and carbonized at 800°C for 4 h	1370	Dynamic test; Material: 0.05 g SO_2: 1200 ppm Flow rate: 30 mL/min	115	1.3 (at. %)	[67]
Activated biochar made from wood panels from a sorting centre, Canada	Fast pyrolysis (250 kg/h) at 454°C and further activation in presence of CO_2 at 750°C, 850°C and 950°C	750: 450 850: 682 950: 866	Dynamic test Material: 1.5 g SO_2: 150 ppm Flow rate: 30 mL/min	347 1117 2138	3.8 3 2.4	**This work**

Note: *CNH: Carbon nanohorns; MWNT: Multiwalled carbon nanotubes; SWNT: Single-walled carbon nanotubes; VACNT: Vertically aligned carbon nanotubes; GO: Graphene oxide.

4 Conclusion

The objective of the present study was to evaluate the fast pyrolysis followed by activation to produce high value-added carbon materials from particleboard waste and assess their potential as adsorbents of SO_2 gas contaminants. For this purpose, melamine particleboards were pyrolyzed at 450°C and subsequently activated at 750°C, 850°C and 950°C in the presence of CO_2. Particleboard waste had a very high nitrogen content of 4.3% due to the presence of urea-formaldehyde and melamine-formaldehyde glue and 94% of this nitrogen was in the form of pyrrolic-N (N-5). Unlike the other studies that employed slow pyrolysis processes at a laboratory scale, the present study applied fast pyrolysis at a pilot scale (CarbonFX, 450°C, 2 s). Under such conditions, all components of the particleboard waste, including the UF and MF resin, were sufficiently thermally degraded. In fact, the pyrolytic treatment removed approximately 66% of the nitrogen present and produced cleaner biochar compared to the original waste. The released nitrogen was in the form of NO, NH_3, and trimethylamine, detected in small amounts compared to the emitted CO_2. Compared to other types of thermochemical conversion methods (e.g., slow pyrolysis), isocyanic acid and hydrogen cyanide were not detected in this study.

The physical activation treatment in the presence of CO_2 at 950°C allowed the development of the following textural properties for the biochar: 866 m^2/g specific surface area, 0.411 cm^3/g total pore volume, 0.272 cm^3/g micropore volume and 0.139 cm^3/g mesopore volume. A non-negligible amount of nitrogen remained in the activated biochars (up to 2.4%) after pyrolysis that was followed by activation, even though much of the nitrogen was devolatilized into liquid and gas. The nitrogen present in these activated biochars was mainly in the form of pyrrolic-N (N-5) and pyridinic-N (N-6). The gas emitted during biochar activation was mainly composed of aromatic hydrocarbon compounds, particularly toluene and benzene, which were detected for the three different activation temperatures, as well as for two nitrogenous species, namely nitric oxide and ethylenediamine. Indeed, the generated activated biochars showed better SO_2 adsorption capacities than the commercial activated carbon (Darco G-60) and the activated biochars made from wood from sawmills. The maximum adsorption capacities of the above materials were up to 2138, 65 and 77 mg/g for a breakthrough time of 19.4, 1.4 and 1.3 h, respectively. However, there is a limitation to the comparison of the results from this study with other studies of N-doped materials available in the literature because of varying adsorption conditions. According to these studies, the presence of nitrogen, the microporosity and high specific surface areas are important parameters for improved adsorption capacity of activated biochars made from particleboard panels. Hence, this study will guide the actions envisaged by Canadian residual materials management policies, which are part of the plan to build a green economy.

Acknowledgement: The authors express their great appreciation to the laboratory personnel of the Industrial Waste Technology Centre (CTRI) for technical assistance.

Funding Statement: This research was funded by the Ministère de l'Économie, de la Science et de l'Innovation du Québec, the Natural Sciences and Engineering Research Council of Canada (NSERC), the Consortium de recherche et innovations en bioprocédés industriels au Québec (Cribiq), the Canada Research Chair Program, the College of Abitibi-Témiscamingue, and the Industrial Waste Technology Centre (Centre Technologique des Résidus Industriels) through its partner on this project, Airex Energy.

Conflicts of Interest: The authors declare that they have no conflicts of interest to report regarding the present study.

References

1. Kelleher, M. (2020). *Preliminary resource recovery report card and gaps assessment for Canada*. Toronto, Canada: Kelleher Environmental.
2. Bhuiyan, M. (2016). Wood: Nonstructural panels. *Reference Module in Materials Science and Materials Engineering, 8*. https://doi.org/10.1016/B978-0-12-803581-8.02221-9
3. Stark, N. M., Cai, Z., Carll, C. (2010). Wood-based composite materials: Panel products, glued-laminated timber, structural composite lumber, and wood-nonwood composite materials. In: *Wood handbook: Wood as an engineering material: Chapter 11*. vol. 190, pp. 11.1–11.28. Madison, WI: US Department of Agriculture, Forest Service, Forest Products Laboratory.
4. Vanreppelen, K., Schreurs, S., Kuppens, T., Thewys, T., Carleer, R. et al. (2013). Activated carbon by co-pyrolysis and steam activation from particle board and melamine formaldehyde resin: Production, adsorption properties and techno economic evaluation. *Journal of Sustainable Development of Energy, Water and Environment Systems, 1(1),* 41–57. https://doi.org/10.13044/j.sdewes.2013.01.0004
5. Government of Canada (2022). 2030 emissions reduction plan–Canada's next steps for clean air and a strong economy. https://www.canada.ca/en/environment-climate-change/news/2022/03/2030-emissions-reduction-plan–canadas-next-steps-for-clean-air-and-a-strong-economy.html
6. Feng, Y., Mu, J., Chen, S., Huang, Z., Yu, Z. (2012). The influence of urea formaldehyde resins on pyrolysis characteristics and products of wood-based panels. *BioResources, 7(4),* 4600–4613. https://doi.org/10.15376/biores.7.4.4600-4613
7. Zhou, L., Shao, Y., Liu, J., Ye, Z., Zhang, H. et al. (2014). Preparation and characterization of magnetic porous carbon microspheres for removal of methylene blue by a heterogeneous fenton reaction. *ACS Applied Materials & Interfaces, 6(10),* 7275–7285. https://doi.org/10.1021/am500576p
8. Nazaret, P. P. (2013). *Bannissement du bois de l'élimination: Le cas du secteur crd, des ici et des zones urbaines et municipales de l'Estrie (Master Thesis)*. Université de Sherbrooke, Québec, Canada and Université de Technologie de Troyes, France. https://savoirs.usherbrooke.ca/bitstream/handle/11143/7349/cufe_Nazaret_P__2014-01-13_essai381.pdf?sequence=1&isAllowed=y.
9. Kan, A. (2009). General characteristics of waste management: A review. *Energy Education Science and Technology Part A: Energy Science and Research, 23(1),* 55–69.
10. Gutierrez, M. J. F., Baxter, D., Hunter, C., Svoboda, K. (2005). Nitrous oxide (N_2O) emissions from waste and biomass to energy plants. *Waste Management & Research: The Journal for a Sustainable Circular Economy, 23(2),* 133–147. https://doi.org/10.1177/0734242X05052803
11. Ribeiro, A. B., Mateus, E. P., Ottosen, L. M., Bech-Nielsen, G. (2000). Electrodialytic removal of Cu, Cr, and as from chromated copper arsenate-treated timber waste. *Environmental Science & Technology, 34(5),* 784–788. https://doi.org/10.1021/es990442e
12. Christensen, I. V., Pedersen, A. J., Ottosen, L. M., Ribeiro, A. B. (2006). Electrodialytic remediation of CCA-treated waste wood in a 2 m^3 pilot plant. *Science of the Total Environment, 364(1–3),* 45–54. https://doi.org/10.1016/j.scitotenv.2005.11.018
13. Sierra-Alvarez, R. (2007). Fungal bioleaching of metals in preservative-treated wood. *Process Biochemistry, 42(5),* 798–804. https://doi.org/10.1016/j.procbio.2007.01.019
14. Chang, Y. C., Choi, D., Kikuchi, S. (2012). Enhanced extraction of heavy metals in the two-step process with the mixed culture of *Lactobacillus bulgaricus* and *Streptococcus thermophilus*. *Bioresource Technology, 103(1),* 477–480. https://doi.org/10.1016/j.biortech.2011.09.059
15. Kakitani, T., Hata, T., Kajimoto, T., Imamura, Y. (2006). Designing a purification process for chromium-, copper- and arsenic-contaminated wood. *Waste Management, 26(5),* 453–458. https://doi.org/10.1016/j.wasman.2005.05.006
16. Janin, A., Blais, J. F., Mercier, G., Drogui, P. (2009). Optimization of a chemical leaching process for decontamination of CCA-treated wood. *Journal of Hazardous Materials, 169(1–3),* 136–145. https://doi.org/10.1016/j.jhazmat.2009.03.064

17. Girods, P., Dufour, A., Rogaume, Y., Rogaume, C., Zoulalian, A. (2008). Thermal removal of nitrogen species from wood waste containing urea formaldehyde and melamine formaldehyde resins. *Journal of Hazardous Materials, 159(2–3),* 210–221. https://doi.org/10.1016/j.jhazmat.2008.02.003
18. Girods, P., Dufour, A., Rogaume, Y., Rogaume, C., Zoulalian, A. (2008). Pyrolysis of wood waste containing urea-formaldehyde and melamine-formaldehyde resins. *Journal of Analytical and Applied Pyrolysis, 81(1),* 113–120. https://doi.org/10.1016/j.jaap.2007.09.007
19. Girods, P., Dufour, A., Fierro, V., Rogaume, Y., Rogaume, C. et al. (2009). Activated carbons prepared from wood particleboard wastes: Characterisation and phenol adsorption capacities. *Journal of Hazardous Materials, 166(1),* 491–501. https://doi.org/10.1016/j.jhazmat.2008.11.04
20. Feng, Y. S., Chen, S. H., Mu, J. (2010). Characterization of products from pyrolysis of waste wood-based composites containing urea-formaldehyde resins. *Advanced Materials Research, 139–141,* 185–189. https://doi.org/10.4028/www.scientific.net/AMR.139-141.185
21. Foong, S. Y., Liew, R. K., Lee, C. L., Tan, W. P., Peng, W. et al. (2022). Strategic hazard mitigation of waste furniture boards via pyrolysis: Pyrolysis behavior, mechanisms, and value-added products. *Journal of Hazardous Materials, 421,* 126774. https://doi.org/10.1016/j.jhazmat.2021.126774
22. Braghiroli, F. L., Bouafif, H., Neculita, C. M., Koubaa, A. (2020). Influence of pyro-gasification and activation conditions on the porosity of activated biochars: A literature review. *Waste and Biomass Valorization, 11(9),* 5079–5098. https://doi.org/10.1007/s12649-019-00797-5
23. Rybiński, P., Syrek, B., Szwed, M., Bradło, D., Żukowski, W. (2021). Influence of thermal decomposition of wood and wood-based materials on the state of the atmospheric air. Emissions of toxic compounds and greenhouse gases. *Energies, 14(11),* 3247. https://doi.org/10.3390/en14113247
24. Puettmann, M., Sahoo, K., Wilson, K., Oneil, E. (2020). Life cycle assessment of biochar produced from forest residues using portable systems. *Journal of Cleaner Production, 250,* 119564. https://doi.org/10.1016/j.jclepro.2019.119564
25. Dong, J., Tang, Y., Nzihou, A., Chi, Y., Weiss-Hortala, E. et al. (2018). Life cycle assessment of pyrolysis, gasification and incineration waste-to-energy technologies: Theoretical analysis and case study of commercial plants. *Science of the Total Environment, 626,* 744–753. https://doi.org/10.1016/j.scitotenv.2018.01.151
26. Hu, G., Feng, H., He, P., Li, J., Hewage, K. et al. (2020). Comparative life-cycle assessment of traditional and emerging oily sludge treatment approaches. *Journal of Cleaner Production, 251,* 119594. https://doi.org/10.1016/j.jclepro.2019.119594
27. Thakur, A. K., Kurtyka, K., Majumder, M., Yang, X., Ta, H. Q. et al. (2022). Recent advances in boron- and nitrogen-doped carbon-based materials and their various applications. *Advanced Materials Interfaces, 9(11),* 2101964. https://doi.org/10.1002/admi.202101964
28. Choudhary, R., Pandey, O. P., Brar, L. K. (2022). Influence of thermal treatment atmosphere on N-doped carbon spheres for wastewater treatment and supercapacitor applications. *Materials Chemistry and Physics, 284,* 126037. https://doi.org/10.1016/j.matchemphys.2022.126037
29. Li, X., Wang, H., Robinson, J. T., Sanchez, H., Diankov, G. et al. (2009). Simultaneous nitrogen doping and reduction of graphene oxide. *Journal of the American Chemical Society, 131(43),* 15939–15944. https://doi.org/10.1021/ja907098f
30. Chen, Z., Higgins, D., Tao, H., Hsu, R. S., Chen, Z. (2009). Highly active nitrogen-doped carbon nanotubes for oxygen reduction reaction in fuel cell applications. *The Journal of Physical Chemistry C, 113(49),* 21008–21013. https://doi.org/10.1021/jp908067v
31. Lim, S., Yoon, S. H., Mochida, I., Jung, D. H. (2009). Direct synthesis and structural analysis of nitrogen-doped carbon nanofibers. *Langmuir, 25(14),* 8268–8273. https://doi.org/10.1021/la900472d
32. Subramanian, N. P., Li, X., Nallathambi, V., Kumaraguru, S. P., Colon-Mercado, H. et al. (2009). Nitrogen-modified carbon-based catalysts for oxygen reduction reaction in polymer electrolyte membrane fuel cells. *Journal of Power Sources, 188(1),* 38–44. https://doi.org/10.1016/j.jpowsour.2008.11.087
33. Choi, C. H., Park, S. H., Woo, S. I. (2012). Phosphorus-nitrogen dual doped carbon as an effective catalyst for oxygen reduction reaction in acidic media: Effects of the amount of P-doping on the physical and

electrochemical properties of carbon. *Journal of Materials Chemistry, 22(24),* 12107. https://doi.org/10.1039/c2jm31079a

34. Braghiroli, F. L., Fierro, V., Izquierdo, M. T., Parmentier, J., Pizzi, A. et al. (2012). Nitrogen-doped carbon materials produced from hydrothermally treated tannin. *Carbon, 50(15),* 5411–5420. https://doi.org/10.1016/j.carbon.2012.07.027
35. Liu, H., Kim, G., Hong, C. O., Song, Y. C., Lee, W. K. et al. (2021). Treatment of phenol wastewater using nitrogen-doped magnetic mesoporous hollow carbon. *Chemosphere, 271,* 129595. https://doi.org/10.1016/j.chemosphere.2021.129595
36. Mohseni, M., Utsch, N., Marcks, C., Demeestere, K., Du Laing, G. et al. (2021). Freestanding nitrogen-doped carbons with hierarchical porosity for environmental applications: A green templating route with bio-based precursors. *Global Challenges, 5(11),* 2100062. https://doi.org/10.1002/gch2.202100062
37. Kasera, N., Kolar, P., Hall, S. G. (2022). Nitrogen-doped biochars as adsorbents for mitigation of heavy metals and organics from water: A review. *Biochar, 4(1),* 17. https://doi.org/10.1007/s42773-022-00145-2
38. Sun, Z., Wang, M., Fan, J., Zhou, Y., Zhang, L. (2020). Regeneration performance of activated carbon for desulfurization. *Applied Sciences, 10(17),* 6107. https://doi.org/10.3390/app10176107
39. Qu, Z., Sun, F., Liu, X., Gao, J., Qie, Z. et al. (2018). The effect of nitrogen-containing functional groups on SO_2 adsorption on carbon surface: Enhanced physical adsorption interactions. *Surface Science, 677,* 78–82. https://doi.org/10.1016/j.susc.2018.05.019
40. Sun, F., Gao, J., Liu, X., Yang, Y., Wu, S. (2016). Controllable nitrogen introduction into porous carbon with porosity retaining for investigating nitrogen doping effect on SO_2 adsorption. *Chemical Engineering Journal, 290,* 116–124. https://doi.org/10.1016/j.cej.2015.12.044
41. Nguyen, M. V., Lee, B. K. (2016). A novel removal of CO_2 using nitrogen doped biochar beads as a green adsorbent. *Process Safety and Environmental Protection, 104,* 490–498. https://doi.org/10.1016/j.psep.2016.04.007
42. Başer, B., Yousaf, B., Yetis, U., Abbas, Q., Kwon, E. E. et al. (2021). Formation of nitrogen functionalities in biochar materials and their role in the mitigation of hazardous emerging organic pollutants from wastewater. *Journal of Hazardous Materials, 416,* 126131. https://doi.org/10.1016/j.jhazmat.2021.126131
43. Girods, P., Rogaume, Y., Dufour, A., Rogaume, C., Zoulalian, A. (2008). Low-temperature pyrolysis of wood waste containing urea–formaldehyde resin. *Renewable Energy, 33(4),* 648–654. https://doi.org/10.1016/j.jhazmat.2021.126131
44. Braghiroli, F. L., Bouafif, H., Hamza, N., Bouslimi, B., Neculita, C. M. et al. (2018). The influence of pilot-scale pyro-gasification and activation conditions on porosity development in activated biochars. *Biomass and Bioenergy, 118,* 105–114. https://doi.org/10.1016/j.biombioe.2018.08.016
45. Brunauer, S., Emmett, P. H., Teller, E. (1938). Adsorption of gases in multimolecular layers. *Journal of the American Chemical Society, 60(2),* 309–319. https://doi.org/10.1021/ja01269a023
46. Dubinin, M. M. (1989). Fundamentals of the theory of adsorption in micropores of carbon adsorbents: Characteristics of their adsorption properties and microporous structures. *Carbon, 27(3),* 457–467. https://doi.org/10.1016/0008-6223(89)90078-X
47. Gregg, S. J., Sing, K. S. W. (1982). *Adsorption, surface area, and porosity*, 2nd edition. London, New York: Academic Press.
48. Tarazona, P. (1995). Solid-fluid transition and interfaces with density functional approaches. *Surface Science, 331–333,* 989–994. https://doi.org/10.1016/0039-6028(95)00170-0
49. ASTM Standard D6646–03 (2008). *Test method for determination of the accelerated hydrogen sulfide breakthrough capacity of granular and pelletized activated carbon.* West Conshohocken: ASTM International. https://doi.org/10.1520/D6646-03R14
50. Moreno, A. I., Font, R. (2015). Pyrolysis of furniture wood waste: Decomposition and gases evolved. *Journal of Analytical and Applied Pyrolysis, 113,* 464–473. https://doi.org/10.1016/j.jaap.2015.03.008
51. Zhan, H., Yin, X., Huang, Y., Yuan, H., Wu, C. (2017). NO precursors evolving during rapid pyrolysis of lignocellulosic industrial biomass wastes. *Fuel, 207,* 438–448. https://doi.org/10.1016/j.fuel.2017.06.046

52. Jin, X. J., Zhang, M. Y., Wu, Y., Zhang, J., Mu, J. (2013). Nitrogen-enriched waste medium density fiberboard-based activated carbons as materials for supercapacitors. *Industrial Crops and Products, 43,* 617–622. https://doi.org/10.1016/j.indcrop.2012.08.006
53. Lemonon, J., Girods, P., Rogaume, C., Perrin, D., Rogaume, Y. (2014). Nitrogen removal from wood laminated flooring waste by low-temperature pyrolysis. *Waste and Biomass Valorization, 5(2),* 199–209. https://doi.org/10.1007/s12649-013-9212-4
54. Aygün, A., Yenisoy-Karakaş, S., Duman, I. (2003). Production of granular activated carbon from fruit stones and nutshells and evaluation of their physical, chemical and adsorption properties. *Microporous and Mesoporous Materials, 66(2–3),* 189–195. https://doi.org/10.1016/j.micromeso.2003.08.028
55. Lemonon, J. (2013). *Energy and material valorisation of laminate flooring by pyrolysis and gasification (Doctoral Thesis)*. Université de Lorraine, France.
56. Zhan, H., Zhuang, X., Song, Y., Huang, Y., Liu, H. et al. (2018). Evolution of nitrogen functionalities in relation to NO precursors during low-temperature pyrolysis of biowastes. *Fuel, 218,* 325–334. https://doi.org/10.1016/j.fuel.2018.01.049
57. Rodríguez-Reinoso, F., Molina-Sabio, M., González, M. T. (1995). The use of steam and CO_2 as activating agents in the preparation of activated carbons. *Carbon, 33(1),* 15–23. https://doi.org/10.1016/0008-6223(94)00100-E
58. García-Martínez, J., Cazorla-Amorós, D., Linares-Solano, A. (2000). Further evidences of the usefulness of CO_2 adsorption to characterize microporous solids. In: Unger, K. K., Kreysa, G., Baselt, J. P. (Eds.), *Studies in surface science and catalysis*, vol. 128, pp. 485–494. Amsterdam, Netherlands: Elsevier. https://doi.org/10.1016/S0167-2991(00)80054-3
59. Sajjadi, B., Chen, W. Y., Egiebor, N. O. (2019). A comprehensive review on physical activation of biochar for energy and environmental applications. *Reviews in Chemical Engineering, 35(6),* 735–776. https://doi.org/10.1515/revce-2017-0113
60. Jansen, R. J. J., van Bekkum, H. (1995). XPS of nitrogen-containing functional groups on activated carbon. *Carbon, 33,* 1021–1027. https://doi.org/10.1016/0008-6223(95)00030-H
61. Xu, D., Gao, Y., Lin, Z., Gao, W., Zhang, H. et al. (2020). Application of biochar derived from pyrolysis of waste fiberboard on tetracycline adsorption in aqueous solution. *Frontiers in Chemistry, 7,* 943. https://doi.org/10.3389/fchem.2019.00943
62. Wu, Y., Jin, X. J., Zhang, J. (2013). Characteristics of nitrogen-enriched activated carbon prepared from waste medium density fiberboard by potassium hydroxide. *Journal of Wood Science, 59(2),* 133–140. https://doi.org/10.1007/s10086-012-1312-4
63. Zhang, L., Hu, X., Wang, Z., Sun, F., Dorrell, D. G. (2018). A review of supercapacitor modeling, estimation, and applications: A control/management perspective. *Renewable and Sustainable Energy Reviews, 81,* 1868–1878. https://doi.org/10.1016/j.rser.2017.05.283
64. Zhan, H., Zhuang, X., Song, Y., Liu, J., Li, S. et al. (2019). A review on evolution of nitrogen-containing species during selective pyrolysis of waste wood-based panels. *Fuel, 253,* 1214–1228. https://doi.org/10.1016/j.fuel.2019.05.122
65. Mu, J., Lai, Z. (2017). Pyrolysis characteristics of wood-based panels and its products. In: Samer, M. (Ed.), *Pyrolysis*. Austria: InTechOpen. https://doi.org/10.5772/67506
66. Girods, P. (2008). *Procédé multi-étagé de valorisation de déchets bois type panneaux de particules (Doctoral Thesis)*. Université Henri Poincaré-Nancy 1, France.
67. Wang, Q., Han, L., Wang, Y., He, Z., Meng, Q. et al. (2022). Conversion of coal into N-doped porous carbon for high-performance SO_2 adsorption. *RSC Advances, 12(32),* 20640–20648. https://doi.org/10.1039/D2RA03098E
68. Braghiroli, F. L., Bouafif, H., Koubaa, A. (2019). Enhanced SO_2 adsorption and desorption on chemically and physically activated biochar made from wood residues. *Industrial Crops and Products, 138,* 111456. https://doi.org/10.1016/j.indcrop.2019.06.019
69. Leng, L., Xu, S., Liu, R., Yu, T., Zhuo, X. et al. (2020). Nitrogen containing functional groups of biochar: An overview. *Bioresource Technology, 298,* 122286. https://doi.org/10.1016/j.biortech.2019.122286

70. Wu, Y., Jin, X. J., Zhang, M. Y., Xu, D. (2012). Phenol adsorption on nitrogen-enriched activated carbon from wood fiberboard waste. *Wood and Fiber Science, 44,* 220–226.
71. Wu, Y., Zhang, J., Jin, X. J., Gao, J. M., Zhao, Q. (2014). Study of Cr(VI) adsorption onto nitrogen-enriched activated carbon from waste medium density fiberboard. *Wood Science and Technology, 48(4),* 713–725. https://doi.org/10.1007/s00226-014-0632-5
72. Liu, W., Adanur, S. (2014). Desulfurization properties of activated carbon fibers. *Journal of Engineered Fibers and Fabrics, 9(2)*. https://doi.org/10.1177/155892501400900208
73. Chen, C., Kim, J., Ahn, W. S. (2012). Efficient carbon dioxide capture over a nitrogen-rich carbon having a hierarchical micro-mesopore structure. *Fuel, 95,* 360–364. https://doi.org/10.1016/j.fuel.2011.10.072
74. Le-Minh, N., Sivret, E. C., Shammay, A., Stuetz, R. M. (2018). Factors affecting the adsorption of gaseous environmental odors by activated carbon: A critical review. *Critical Reviews in Environmental Science and Technology, 48(4),* 341–375. https://doi.org/10.1080/10643389.2018.1460984
75. Liu, W. (2010). *Activated carbon fiber filter media for proton exchange membrane fuel cell (Doctoral Thesis)*. Auburn University, Alabama, USA.
76. Li, H., Zhang, J., Cao, Y., Liu, C., Li, F. et al. (2020). Role of acid gases in Hg^0 removal from flue gas over a novel cobalt-containing biochar prepared from harvested cobalt-enriched phytoremediation plant. *Fuel Processing Technology, 207,* 106478. https://doi.org/10.1016/j.fuproc.2020.106478
77. Li, H., Zhang, J., Cao, Y., Wang, Y., Li, F. et al. (2021). Capture of elemental mercury from flue gas over a magnetic and sulfur-resistant sorbent prepared from Fe-containing sewage sludge activated with sulfuric acid. *Fuel, 300,* 120938. https://doi.org/10.1016/j.fuel.2021.120938
78. Atanes, E., Nieto-Márquez, A., Cambra, A., Ruiz-Pérez, M. C., Fernández-Martínez, F. (2012). Adsorption of SO_2 onto waste cork powder-derived activated carbons. *Chemical Engineering Journal, 211–212,* 60–67. https://doi.org/10.1016/j.cej.2012.09.043
79. Chen, A., Yu, Y., Zhang, Y., Zang, W., Yu, Y. et al. (2014). Aqueous-phase synthesis of nitrogen-doped ordered mesoporous carbon nanospheres as an efficient adsorbent for acidic gases. *Carbon, 80,* 19–27. https://doi.org/10.1016/j.carbon.2014.08.003
80. Shao, J., Zhang, J., Zhang, X., Feng, Y., Zhang, H. et al. (2018). Enhance SO_2 adsorption performance of biochar modified by CO_2 activation and amine impregnation. *Fuel, 224,* 138–146. https://doi.org/10.1016/j.fuel.2018.03.064
81. Wang, A., Fan, R., Pi, X., Zhou, Y., Chen, G. et al. (2018). Nitrogen-doped microporous carbons derived from pyridine ligand-based metal–organic complexes as high-performance SO_2 adsorption sorbents. *ACS Applied Materials & Interfaces, 10,* 37407–37416. https://doi.org/10.1021/acsami.8b12739
82. Babu, D. J., Puthusseri, D., Kühl, F. G., Okeil, S., Bruns, M. et al. (2018). SO_2 gas adsorption on carbon nanomaterials: A comparative study. *Beilstein Journal of Nanotechnology, 9,* 1782–1792. https://doi.org/10.3762/bjnano.9.169
83. Wang, A., Fan, R., Pi, X., Hao, S., Zheng, X. et al. (2019). N-doped porous carbon derived by direct carbonization of metal–organic complexes crystal materials for SO_2 adsorption. *Crystal Growth & Design, 19(3),* 1973–1984. https://doi.org/10.1021/acs.cgd.8b01925

Appendix

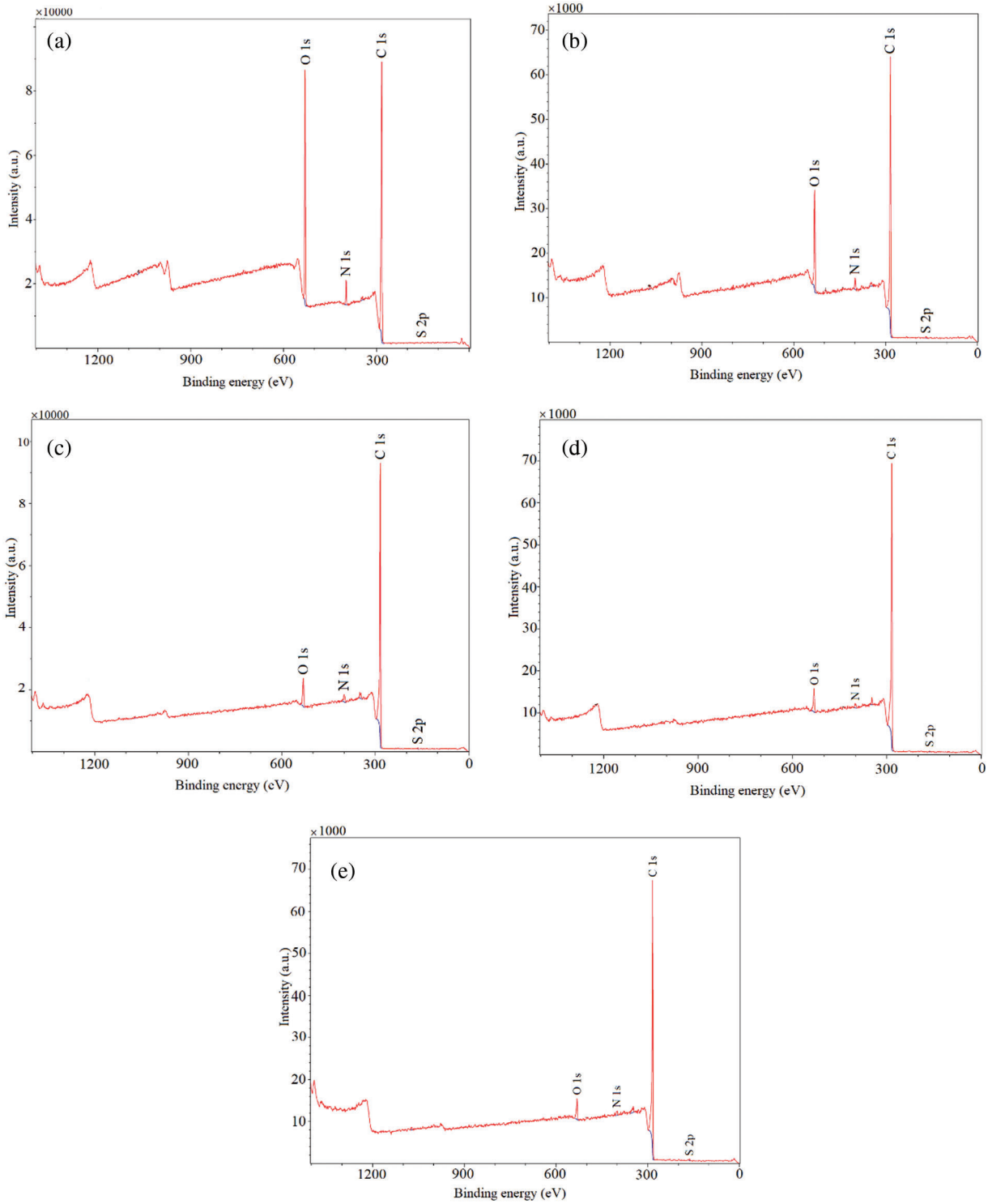

Figure S1: X-ray photoelectron spectroscopy (XPS) spectra of: (a) Wood panels; (b) Wood panels pyrolyzed at 450°C; and then activated at (c) 750°C; (d) 850°C and (e) 950°C

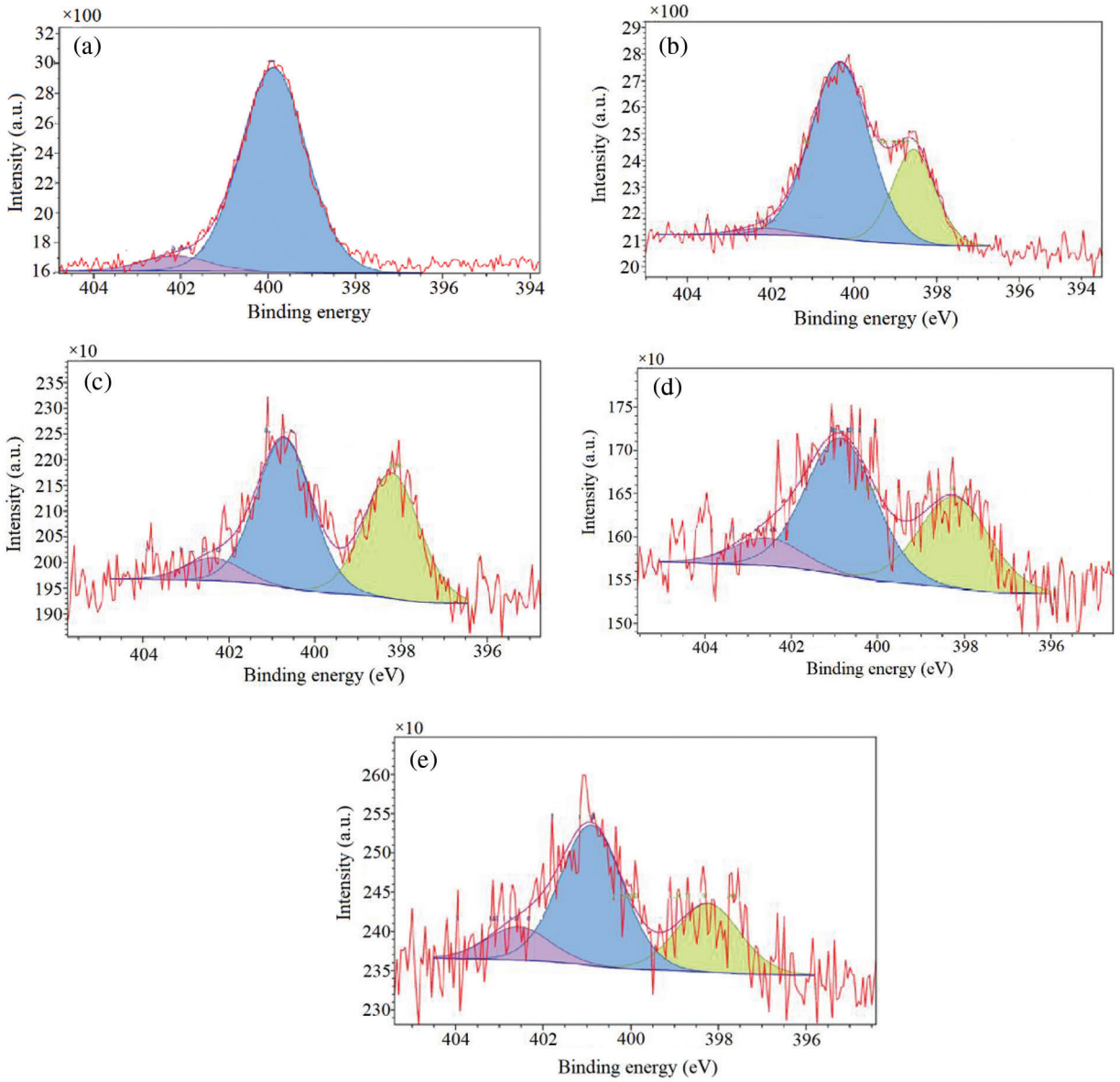

Figure S2: Deconvoluted N 1s X-ray photoelectron spectroscopy (XPS) spectrum of: (a) Wood panels; (b) Wood panels pyrolyzed at 450°C; and then activated at (c) 750°C; (d) 850°C and (e) 950°C